Influence of carrier-carrier and carrier-phonon correlations on optical absorption and gain in quantum-dot systems

M. Lorke,[1,*] T. R. Nielsen,[1] J. Seebeck,[1] P. Gartner,[1,2] and F. Jahnke[1]
[1]*Institute for Theoretical Physics, University of Bremen, 28334 Bremen, Germany*
[2]*National Institute for Materials Physics, POB MG-7, Bucharest-Magurele, Romania*
(Received 21 September 2005; revised manuscript received 13 January 2006; published 28 February 2006)

A microscopic theory is used to study the optical properties of semiconductor quantum dots. The dephasing of a coherent excitation and line shifts of the interband transitions due to carrier-carrier Coulomb interaction and carrier-phonon interaction are determined from a quantum kinetic treatment of correlation processes. We investigate the density dependence of both mechanisms and clarify the importance of various dephasing channels involving the localized and delocalized states of the system.

DOI: 10.1103/PhysRevB.73.085324 PACS number(s): 78.67.Hc, 71.35.Cc

I. INTRODUCTION

In recent years, semiconductor quantum dots (QDs) have been studied extensively due to possible applications in optoelectronic devices like LEDs, lasers, or amplifiers.[1,2] In the rapidly emerging field of quantum information technology, QDs have been successfully used to demonstrate the generation of single photons or correlated photon pairs.[3–5] Furthermore, the strong coupling regime for QD emitters in optical microcavities has been demonstrated.[6,7] A common aspect in fundamental studies and practical applications of QDs is the critical role of dephasing processes. They determine the homogeneous linewidth of the QD resonances, limit the coherence properties of QD lasers and their ultrafast emission dynamics, and have a strong influence on coherent optical nonlinearities. Moreover, dephasing processes are intimately linked to line shifts of the QD resonances.

Optical studies of QDs have been recently focused on self-assembled systems that are typically grown in the Stranski-Krastanoff mode. The resulting QDs are randomly distributed on a two-dimensional wetting layer (WL). The interplay of carriers in the localized QD and delocalized WL states is mediated by the Coulomb interaction of carriers in addition to carrier-phonon interaction.

Theoretical studies of absorption and gain in QDs have been accomplished on the basis of multilevel optical Bloch equations,[8] or semiconductor Bloch equations (SBE) with screened exchange and Coulomb hole contributions.[9] However, in these approaches the dephasing is merely a parameter entering the calculation via a T_2 time. In Ref. 10 the dephasing due to Coulomb interaction has been calculated using SBE with correlation contributions due to Auger-like WL-assisted capture processes (see below) where scattering integrals have been evaluated in terms of free-carrier energies. A more elaborate analysis of dephasing due to Coulomb interaction in quantum wells (QWs), which included non-Markovian scattering integrals based on renormalized energies, revealed quantitative modifications of the results.[11] We show that for QD systems the situation is different due to the appearance of localized states with a discrete spectrum. The calculation of scattering integrals in terms of free-carrier energies breaks down for processes due to the Coulomb interactions that involve only localized states. It turns out that these are among the dominant processes for QDs containing more than one confined shell. For other processes involving localized states, their energy renormalization is also of enhanced importance. In the first part of this paper we present a non-Markovian treatment of dephasing due to a Coulomb interaction, where energy renormalizations under high-density conditions typical for QD lasers are self-consistently included and the importance of various scattering channels is analyzed.

For the interaction of QD carriers with LA phonons, extensive work has been devoted to the low-temperature regime.[12–14] It is generally acknowledged that acoustic phonons dominate the dephasing at low temperatures. Nevertheless, several low-temperature PL measurements[16,17] revealed LO-phonon replicas. In Ref. 15 it was suggested that for temperatures above 100 K, the dephasing due to a carrier-LO-phonon interaction is of growing importance. The interaction of QD carriers with LO phonons is strongly influenced by hybridization effects,[18] which require the application of the polaron picture. A quantum-kinetic description of carrier-phonon scattering based on polarons has recently been used to explain ultrafast carrier capture and relaxation processes in QDs.[19] In the second part of this paper, we present the corresponding treatment of dephasing processes. Then the combined influence of the Coulomb interaction and the carrier-phonon interaction on optical absorption and gain spectra is analyzed for quasiequilibrium excitation conditions.

In Refs. 20 and 21 PL spectroscopy measurements revealed homogeneous linewidths of several meV at room temperature. Comparable results have also been found by four-wave mixing experiments.[15] Our microscopic calculation can reproduce these experimental findings, even though a direct quantitative comparison, which is not our purpose in this paper, would require better knowledge of the specific QD parameters as well as possible improvements of our QD model.

Our primary focus in this work is on QD optical spectra in the room-temperature high-density regime relevant for laser applications. For this situation, a quantum kinetic theory for carrier-carrier interaction and carrier scattering with LO

phonons is developed. It is shown that non-Markovian effects and energy renormalizations play an essential role in QD systems. The theory is evaluated to compare the contributions of various scattering channels to dephasing and line shifts as well as their excitation density dependence. Studies of the temperature dependence are restricted to $T \geqslant 150$ K, where the inclusion of LA phonons is not necessary.

Our investigations show that the efficiency of dephasing processes depends strongly on the carrier density in the system. For low carrier densities and room temperature, the electron-LO-phonon interaction is the dominant mechanism, leading to the appearance of additional side peaks in the optical spectra due to polaronic hybridization effects. Even though for high carrier densities the Coulomb interaction becomes the dominant mechanism, the electron-LO-phonon interaction remains important, as it continues to contribute to the linewidth and line shape of the QD resonances.

For typical InGaAs QD parameters, a QD density of 10^{10} cm^{-2} on the WL and carrier densities around 10^{10} cm^{-2} at room temperature, we obtain a homogeneous linewidth of the ground state resonance with a full width at half-maximum (FWHM) of 3.2 meV, in agreement with the experimental findings of Ref. 20. For lower carrier densities and decreasing temperature, we can reproduce the observed dephasing reduction while for elevated carrier densities and decreasing temperature, the reduction of the dephasing due to LO phonons is compensated by increasing dephasing due to Coulomb scattering.

II. THEORY OF OPTICAL ABSORPTION AND GAIN CALCULATIONS

The coherent optical excitation of semiconductors can be described in terms of interband transition amplitudes $\psi_\alpha = \langle e_\alpha h_\alpha \rangle$ and population functions $f_\alpha^e = \langle e_\alpha^\dagger e_\alpha \rangle$ and $f_\alpha^h = \langle h_\alpha^\dagger h_\alpha \rangle$ for electrons and holes, respectively. For the annihilation and creation operators of electrons and holes, α combines the quantum numbers for either WL or QD states. The dynamics of $\psi_\alpha(t)$ and $f_\alpha^{e,h}(t)$ in response to the optical field $E(t)$ is determined by the SBE,[22] which can be used to incorporate many-body interaction effects to describe dephasing, energy renormalization, and screening, as demonstrated for QWs in Ref. 23. The optical absorption or gain coefficient can be defined via the response of the system to a weak optical field $E(\omega)$ in terms of the linear optical susceptibility $\chi(\omega) = P(\omega)/E(\omega)$. Here $P(\omega)$ is the Fourier transform of the macroscopic polarization $P(t) = \Sigma_\alpha d_\alpha^* \psi_\alpha$ with the interband dipole matrix element d_α.

A solution linear in the optical probe field $E(t)$ implies that changes of the electron and hole population $f_\alpha^{e,h}$ due to $E(t)$ can be neglected. In the following we consider quasi-equilibrium distributions for electron and holes that are approximately realized in injection-current-driven devices. Alternatively the carriers can be generated with an optical prepulse, where a sufficient delay of the probe pulse ensures that the excited carriers are thermalized and that coherent effects of the pump pulse can be neglected.

In this regime, the Fourier transform of the coherent interband transition amplitude ψ_α obeys the equation

$$(\hbar\omega - \varepsilon_\alpha^{e,\mathrm{HF}} - \varepsilon_\alpha^{h,\mathrm{HF}})\psi_\alpha(\hbar\omega) + [1 - f_\alpha^e - f_\alpha^h]\Omega_\alpha^{\mathrm{HF}}(\hbar\omega) = S_\alpha^{\mathrm{Coul}}(\hbar\omega) + S_\alpha^{\mathrm{Phon}}(\hbar\omega). \quad (1)$$

The single-particle energies entering Eq. (1) include already renormalizations due to Hartree-Fock (HF) Coulomb effects according to $\varepsilon_\alpha^{a,\mathrm{HF}} = e_\alpha^a + \Sigma_\alpha^{a,\mathrm{HF}}$, with $a = e, h$. Here e_α^a are the free-carrier energies and $\Sigma_\alpha^{a,\mathrm{HF}} = \Sigma_\beta (V_{\alpha\beta\beta\alpha} - V_{\alpha\beta\alpha\beta}) f_\beta^a$ combines the Hartree and exchange Coulomb self-energy. In a spatially homogeneous system like bulk semiconductors or for the in-plane motion for QWs, the Hartree terms cancel due to local charge neutrality. In the QD-WL system, the absence of local charge neutrality leads to Hartree contributions for the QD states. The influence of the WL states can be incorporated approximately within screened QD Hartree contributions, as discussed in detail in Ref. 24. The Coulomb exchange contributions to the interband Rabi energy $\Omega_\alpha^{\mathrm{HF}}(\hbar\omega) = \boldsymbol{d}\cdot\boldsymbol{E}(\hbar\omega) + \Sigma_\beta V_{\alpha\beta\alpha\beta}\psi_\beta(\hbar\omega)$ give rise to the excitonic resonance of the WL and QD states.

Without the terms $S_\alpha^{\mathrm{Coul}}(\hbar\omega)$ and $S_\alpha^{\mathrm{Phon}}(\hbar\omega)$, we would recover the well-known semiconductor Bloch equations[22] formulated in an arbitrary eigenfunction basis. $S_\alpha^{\mathrm{Coul}}(\hbar\omega)$ and $S_\alpha^{\mathrm{Phon}}(\hbar\omega)$ are used to describe correlation contributions that lead to dephasing of the coherent polarization and to the corresponding additional energy renormalizations due to Coulomb interaction and carrier-phonon interaction, respectively. These terms will be discussed in the following sections. A general feature of the following description is that the dephasing contributions for both the Coulomb interaction and the carrier-phonon interaction can be separated into a part that is diagonal in the state index α for the transition amplitude (diagonal dephasing Γ^{DD}) and a corresponding off-diagonal part (Γ^{OD}) that mixes the coherent interband transition amplitudes for various states according to

$$S_\alpha(\hbar\omega) = -\Gamma_\alpha^{\mathrm{DD}}(\hbar\omega)\psi_\alpha(\hbar\omega) + \sum_{\alpha_1} \Gamma_{\alpha\alpha_1}^{\mathrm{OD}}(\hbar\omega)\psi_{\alpha_1}(\hbar\omega). \quad (2)$$

The imaginary part of Γ^{DD} describes a dephasing (damping) of the coherent polarization that can be expressed as a state and frequency dependent T_2 time. The contribution of Γ^{DD} is, however, partly compensated by the off-diagonal contribution Γ^{OD}. The real parts of Γ^{DD} and Γ^{OD} give rise to additional renormalizations of the energies on the lhs of Eq. (1).

III. COULOMB INTERACTION

A. THEORY

The correlation contributions due to Coulomb interaction, $S_\alpha^{\mathrm{Coul}}(\hbar\omega)$, are evaluated in the second-order Born approximation. To close the set of equation for the interband transition amplitude ψ, we additionally apply the generalized Kadanoff-Baym ansatz (GKBA).[25,26] Within this approach the correlation contributions due to Coulomb interaction read as

$$\Gamma_{\alpha}^{\mathrm{DD}}(\hbar\omega) = i \sum_{\substack{a,b=e,h \\ b\neq a}} \sum_{\alpha_1\alpha_2\alpha_3} \times \{W_{\alpha\alpha_2\alpha_3\alpha_1}[2W^{*}_{\alpha\alpha_2\alpha_3\alpha_1} - W^{*}_{\alpha\alpha_2\alpha_1\alpha_3}] \times g(\hbar\omega - \tilde{\varepsilon}^{b}_{\alpha} - \tilde{\varepsilon}^{a}_{\alpha_1} + (\tilde{\varepsilon}^{a}_{\alpha_2})^{*} - \tilde{\varepsilon}^{a}_{\alpha_3})[(1-f^{a}_{\alpha_2})f^{a}_{\alpha_3}f^{a}_{\alpha_1} + (f\to 1-f)] + 2W^{*}_{\alpha\alpha_2\alpha_3\alpha_1}W_{\alpha\alpha_2\alpha_3\alpha_1} \times g(\hbar\omega - \tilde{\varepsilon}^{b}_{\alpha} - \tilde{\varepsilon}^{a}_{\alpha_1} - \tilde{\varepsilon}^{b}_{\alpha_2} + (\tilde{\varepsilon}^{b}_{\alpha_3})^{*})[f^{b}_{\alpha_2}(1-f^{b}_{\alpha_3})f^{a}_{\alpha_1} + (f\to 1-f)]\}, \quad (3)$$

and

$$\Gamma_{\alpha\alpha_1}^{\mathrm{OD}}(\hbar\omega) = i \sum_{\substack{a,b=e,h \\ b\neq a}} \sum_{\alpha_2\alpha_3} \times \{W_{\alpha\alpha_2\alpha_3\alpha_1}[2W^{*}_{\alpha\alpha_2\alpha_3\alpha_1} - W^{*}_{\alpha\alpha_2\alpha_3\alpha_1}] \times g(\hbar\omega - \tilde{\varepsilon}^{a}_{\alpha} - \tilde{\varepsilon}^{b}_{\alpha_1} - \tilde{\varepsilon}^{a}_{\alpha_2} + (\tilde{\varepsilon}^{a}_{\alpha_3})^{*})[(1-f^{a}_{\alpha_3})f^{a}_{\alpha_2}f^{a}_{\alpha} + (f\to 1-f)] + 2W_{\alpha\alpha_2\alpha_3\alpha_1}W^{*}_{\alpha\alpha_2\alpha_3\alpha_1} \times g(\hbar\omega - \tilde{\varepsilon}^{a}_{\alpha} - \tilde{\varepsilon}^{b}_{\alpha_1} + (\tilde{\varepsilon}^{b}_{\alpha_2})^{*} - \tilde{\varepsilon}^{b}_{\alpha_3})[f^{b}_{\alpha_3}(1-f^{b}_{\alpha_2})f^{a}_{\alpha} + (f\to 1-f)]\}, \quad (4)$$

with the screened Coulomb interaction matrix elements $W_{\alpha\alpha_2\alpha_3\alpha_1}$ discussed in Appendix A. Note that $\tilde{\varepsilon}^{a}_{\alpha}=\varepsilon^{a}_{\alpha}-i\gamma^{a}_{\alpha}$ appearing in the function $g(\Delta)=i/\Delta$ are effective complex single-particle energies that combine renormalized energies ε^{a}_{α} as well as the corresponding quasiparticle damping γ^{a}_{α}. This is elaborated in more detail later.

As for the particle scattering[27] we have direct and exchange contributions that are proportional to $2|W_{\alpha\alpha_2\alpha_3\alpha_1}|^2$ and $W_{\alpha\alpha_2\alpha_3\alpha_1}W^{*}_{\alpha\alpha_2\alpha_1\alpha_3}$, respectively. The population factors describe the availability of initial and final states. For the previously discussed excitation conditions, the population factors are time independent and we have restricted ourselves to the contributions linear in the transition amplitude ψ_{α}.

The frequency dependence of Γ^{DD} and Γ^{OD} in Eqs. (3) and (4) reflect the non-Markovian treatment of the dephasing processes. Indeed, in this case, the product of the type $\Gamma\psi$ of Eq. (2) amounts, in the time domain, to a convolution integral describing memory effects. The Markovian limit is obtained by pulling out from this integral the slowly varying component of $\psi_{\alpha}(t)$. Then the fast component $e^{(i/\hbar)(\tilde{\varepsilon}^{a}_{\alpha}+\tilde{\varepsilon}^{b}_{\alpha})t}$ $(a\neq b)$ fixes the frequency value at $\omega=\omega_{\alpha}=(1/\hbar)(\tilde{\varepsilon}^{e}_{\alpha}+\tilde{\varepsilon}^{h}_{\alpha})$ for Γ^{DD} and $\omega=\omega_{\alpha_1}$ for Γ^{OD}, so that in this limit both dephasing contributions become frequency independent (see Appendix C for details). If one combines the Markov approximation with the use of free-carrier energies in the scattering contributions, the diagonal dephasing is given by the sum of in- and outscattering rates, $\mathrm{Im}(\Gamma^{\mathrm{DD}}_{\alpha})=S^{\mathrm{in}}_{\alpha}+S^{\mathrm{out}}_{\alpha}$. Here $S^{\mathrm{in,out}}_{\alpha}$ are the rates in the Markovian kinetic equation for the carrier population, as defined, e.g., in Ref. 27. Results of these equations for optical spectra have been studied in detail for QW systems. If one restricts the analysis to diagonal dephasing contributions Γ^{DD} and neglects off-diagonal dephasing terms Γ^{OD}, damping of the excitonic resonances is grossly overestimated.[23] Non-Markovian calculations further reduce the interaction-induced broadening and line-shift of the excitonic resonances in QW systems.[11]

For the following discussion we would like to point out that one has to compare on one side the Markov approximation with a non-Markovian treatment and on the other side the use of free-carrier energies versus renormalized energies in the scattering integrals. The non-Markovian treatment is more crucial in QD systems compared to QWs, since the discrete part of the spectrum with large energy separation emphasizes the frequency dependence of the dephasing rates.[10]

For the use of free-carrier energies in the scattering contributions, the limit $\gamma^{a}_{\alpha}\to 0, \gamma^{a}_{\alpha}>0$ leads to $g(\Delta)=\pi\delta(\Delta)+iP(1/\Delta)$ where P denotes the principal value integral. This approximation implies serious difficulties in a QD system when processes are taken into account that involve only discrete states. In these cases the δ functions are not integrated out and thus the results are not well defined. Note that this is not an artifact of the Markov approximation but also applies to the non-Markovian calculation. Even if one would introduce a finite broadening of the δ function, e.g., due to the interaction of carriers with acoustic phonons, the non-Markovian calculation still yields unphysical results. This is because the spectrum predicted by Eq. (1) has peaks at the energies of the lhs renormalized by the correlation contributions on the rhs, and hence, $\hbar\omega$ samples renormalized interband transitions. If they are mixed with free-carrier energies in the correlation contributions, Eqs. (3) and (4), via $g(\hbar\omega-\Delta)$, then artificially also free carrier transitions and hybridization effects between all these energies can appear in the optical spectra, which are absent when self-consistently renormalized energies are used.

Another important point, which complicates the treatment of the coupled QD-WL system, is the existence of many scattering channels that are often partly neglected (for a discussion of the scattering channels in the framework of carrier kinetics see Ref. 27). This can strongly influence the results, as we will show in Sec. III B.

1. Self-consistent single-particle energy renormalizations

The renormalization of the single-particle energies, which enter in the dephasing rates, originates from the same interaction processes that determine the dephasing itself. Technically, they can be traced back to the same many-body self-energy. The renormalized energies can be obtained from the poles of the retarded Green's function (GF) in Fourier space. In the absence of interaction, the retarded GF is given by

$$G^{0,\mathrm{ret}}_{a,\alpha}(\hbar\omega) = \frac{1}{\hbar\omega - e^{a}_{\alpha} + i\delta}, \quad (5)$$

with the single-particle energy e^{a}_{α} and $\delta\to 0, \delta>0$. At elevated carries densities, it is a reasonable approximation, that the main effect of the Coulomb interaction is a shift of the single-particle energy and the addition of a quasiparticle broadening such that the single-pole structure of the retarded

GF remains valid. This picture corresponds to the Landau theory of a Fermi liquid and leads to the retarded GF of the interacting system,

$$G^{\mathrm{ret}}_{a,\alpha}(\hbar\omega) = \frac{1}{\hbar\omega - \tilde{\varepsilon}^a_\alpha} = \frac{1}{\hbar\omega - \varepsilon^a_\alpha + i\gamma^a_\alpha}. \tag{6}$$

With this ansatz, we define a complex effective single-particle energy $\tilde{\varepsilon}^a_\alpha = \varepsilon^a_\alpha - i\gamma^a_\alpha$ that consists of a renormalized energy ε^a_α and the corresponding quasiparticle damping γ^a_α. In the pole approximation, the self-consistency requirement leads to

$$\tilde{\varepsilon}^a_\alpha = e^a_\alpha + \Sigma^{a,\mathrm{HF}}_\alpha + \Sigma^{a,\mathrm{ret}}_\alpha(\tilde{\varepsilon}^a_\alpha) \tag{7}$$

with the retarded self-energy

$$\begin{aligned}\Sigma^{a,\mathrm{ret}}_\alpha(\hbar\omega) = -i \sum_{\substack{b=e,h \\ b\neq a}} \sum_{\alpha_1\alpha_2\alpha_3} & \\ \times \{ & W^*_{\alpha\alpha_2\alpha_3\alpha_1}[2W^*_{\alpha\alpha_2\alpha_3\alpha_1} - W^*_{\alpha\alpha_2\alpha_1\alpha_3}] g(\hbar\omega - \tilde{\varepsilon}^a_{\alpha_1} \\ & + (\tilde{\varepsilon}^a_{\alpha_2})^* - \tilde{\varepsilon}^a_{\alpha_3})[(1-f^a_{\alpha_2})f^a_{\alpha_3}f^a_{\alpha_1} + (f \to 1-f)] \\ & + 2W^*_{\alpha\alpha_2\alpha_3\alpha_1} W_{\alpha\alpha_2\alpha_3\alpha_1}\, g(\hbar\omega - \tilde{\varepsilon}^a_{\alpha_1} - \tilde{\varepsilon}^b_{\alpha_2} + (\tilde{\varepsilon}^b_{\alpha_3})^*) \\ & \times [f^b_{\alpha_2}(1-f^b_{\alpha_3})f^a_{\alpha_1} + (f \to 1-f)]\}. \end{aligned} \tag{8}$$

The close connection between the diagonal dephasing and the retarded self-energy $\Sigma^{a,\mathrm{ret}}_\alpha$ can be expressed as

$$\Gamma^{\mathrm{DD}}_\alpha(\hbar\omega) = \sum_{\substack{a,b=e,h \\ b\neq a}} \Sigma^{a,\mathrm{ret}}_\alpha(\hbar\omega - \tilde{\varepsilon}^b_\alpha). \tag{9}$$

B. Results

Throughout this paper, results are presented for a carrier and lattice temperature of 300 K and a density of QDs on the WL of $n_{\mathrm{QD}} = 10^{10}$ cm^{-2}. Further details of the QD model are given in Appendix A.

In Fig. 1 we show optical absorption spectra for the combined QD-WL system and various carrier densities. Excitation-induced dephasing and energy renormalizations due to Coulomb interaction have been included according to Eqs. (3), (4), (7), and (8). Identifiable are the excitonic resonance of the WL at around −15 meV as well as the *p*-shell and *s*-shell resonances at about −90 m and −150 meV, respectively. We observe a strong damping of these resonances with increasing carrier density that is accompanied by a pronounced red shift of the QD lines. The transition from absorption to gain takes place at a density $\sim 1\times10^{11}$ cm^{-2} ($\sim 5\times10^{11}$ cm^{-2}) for the *s* shell (*p* shell). An important point for practical applications is the saturation of the optical gain for the *s* shell accompanied by an increasing red shift. This is due to a combination of state filling and saturation of dephasing at the *s* shell resonance. In contrast the gain at the *p*-shell resonance increases further and shows no saturation for the densities investigated here.

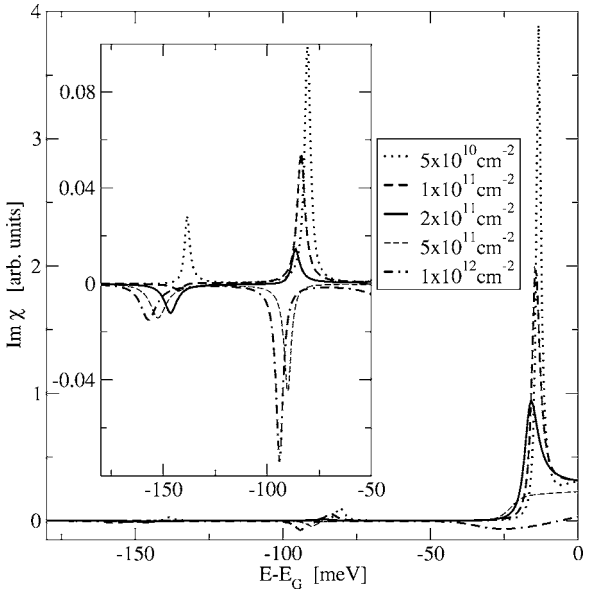

FIG. 1. Imaginary part of the optical susceptibility for the combined QD-WL system including interaction-induced dephasing and line shifts due to the Coulomb interaction for various total carrier densities. The inset shows a scale up of the QD resonances.

1. Importance of different dephasing processes and frequently used approximations

The Coulomb matrix elements allow to distinguish between different dephasing processes in complete analogy to the carrier scattering.[27] If all four indices of $W_{\alpha\alpha_2\alpha_3\alpha_1}$ are WL states, we refer to the corresponding processes as WL relaxation. They describe dephasing and energy shifts of the WL states in the optical spectra. Apart from the fact that we have to include OPW corrections to the interaction matrix elements for a proper description of the coupled QD-WL system,[27] this resembles the case of a QW system. Since the processes involving QD states (except intradot processes, see later) are discussed in great detail in Ref. 27 we will only give a brief survey here.

If one of the four indices of $W_{\alpha\alpha_2\alpha_3\alpha_1}$ corresponds to a QD state, we consider the dephasing mechanism as WL-assisted carrier capture, because in the corresponding scattering process an electron or a hole is captured from the WL to the QD.[27] Likewise, we refer to processes with two QD state indices as WL-assisted relaxation and to processes with three QD state indices as dot-assisted processes. Intradot processes are described when all four indices of $W_{\alpha\alpha_2\alpha_3\alpha_1}$ correspond to QD states. These scattering events are not important in the carrier dynamics, because we only consider two confined shells for electrons and holes and therefore such scattering processes cannot redistribute carriers. However, they clearly provide additional dephasing of the coherent polarization. Note that the intradot processes are not the only events that produce dephasing without the redistribution of carriers. Such processes, in which two carriers switch their states, also appear in the WL-assisted relaxation and in the WL relaxation.

Figure 2 shows that WL-assisted relaxation (dash-dotted line) and intradot scattering (thin solid line), which include

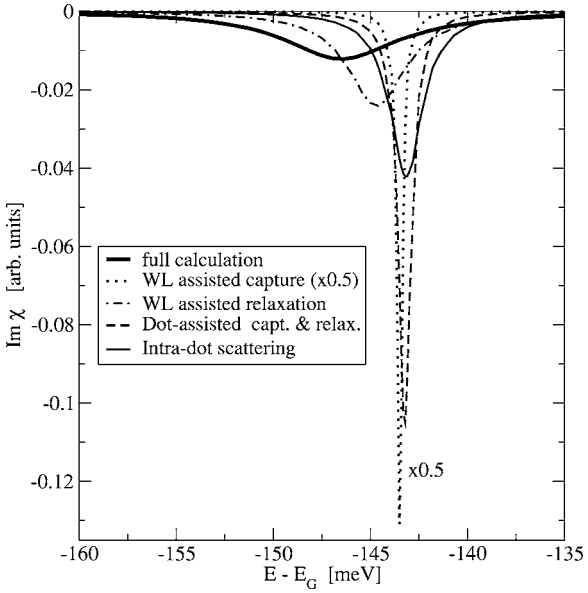

FIG. 2. Imaginary part of the optical susceptibility for the *s*-shell resonances at a carrier density of 2×10^{11} cm^{-2}. The result including all considered Coulomb scattering processes (a thick solid line) is compared to calculations where only certain classes of processes are evaluated.

the processes leading to dephasing without the redistribution of carriers, are the most important contributions, while WL-assisted capture (dotted line) and dot-assisted (dashed line) processes cause a rather small dephasing. However, since this picture can change with carrier density, it is important to test the influence of all dephasing channels.

In Fig. 3 we compare the optical susceptibility from the full calculation (solid line) with a result where only the diagonal dephasing contributions were taken into account (dotted lines). For the excitonic resonance of the WL, the absence of the off-diagonal dephasing leads to a overestimation of the linewidth by roughly a factor of 2 under the considered high-density conditions. Using only the diagonal dephasing contributions turns out to be a reasonable approximation for the lowest QD resonances while for the excited QD transition the lineshape is not fully reproduced. Off-diagonal dephasing contributions are less important for the QD resonances due to the rather large spectral separation between the QD states and the WL states and for the same reason off-diagonal contributions are stronger for the *p* shell than for the *s* shell.

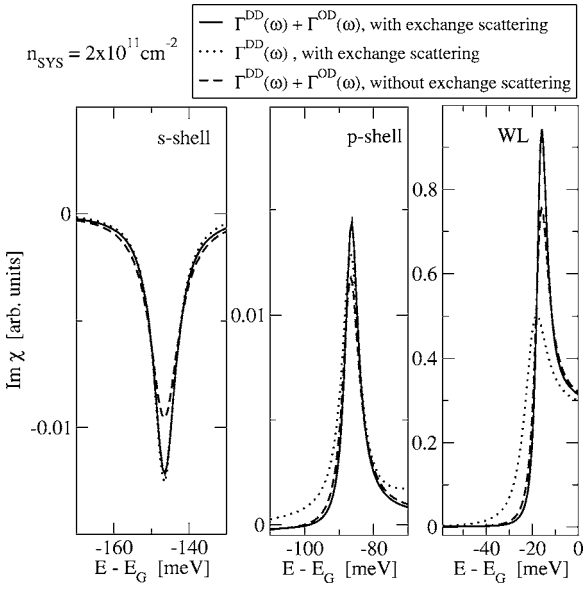

FIG. 3. Imaginary part of the optical susceptibility for a carrier density of 2×10^{11} cm^{-2} with full dephasing contributions (solid lines), with diagonal dephasing contributions (dotted lines), and with diagonal and off-diagonal dephasing but without the exchange scattering in both terms (dashed lines).

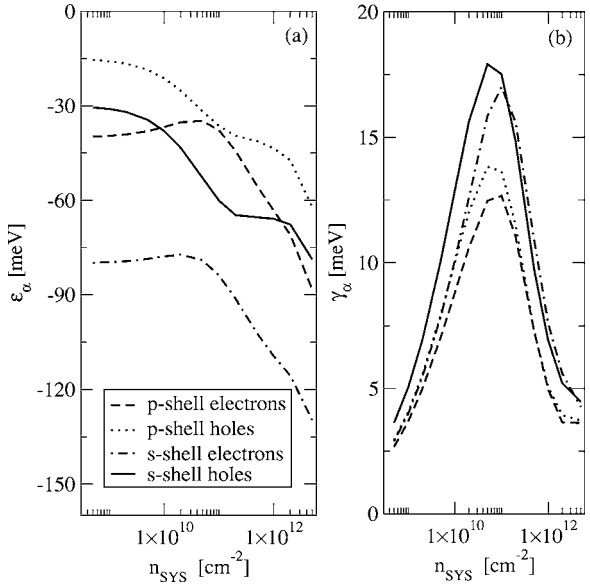

FIG. 4. Renormalized single-particle energies of the QD states for electrons and holes as a function of the total carrier density in the system (a) and corresponding single-particle broadening (b).

Note that the foregoing discussion applies to the non-Markovian treatment. If one neglects the off-diagonal dephasing and uses the Markov approximation, again the dephasing is grossly overestimated when all relevant scattering processes are included. For the discussed QD model, transitions due to localized states are completely damped out in this approximation.

The influence of the exchange term in the dephasing rates, which is often disregarded, is also investigated in Fig. 3. Neglecting the exchange scattering in the dephasing contributions clearly overestimates the homogeneous linewidth by about 30%, thus pointing out that the exchange terms are almost as important as the direct term and should be included in the calculation.

2. Renormalization of single-particle states

As discussed previously, the single particle renormalizations are of critical importance for the proper determination of the dephasing rates. In Fig. 4(a) the single particle renormalizations due to the Coulomb interaction are shown. The

Fock and correlation contributions lead to a decrease of the single-particle energies with increasing carrier density. The Hartree terms increase the energies for electrons and decrease the energies for holes (for a detailed discussion cf. Ref. 24). This leads to slightly increasing (decreasing) single-particle energies for the electrons (holes) from low to intermediate carrier densities. For higher densities, both electron and hole energies strongly decrease.

With increasing carrier densities the single-particle broadening [Fig. 4(b)] strongly grows up to intermediate carrier densities due to the larger availability of scattering partners. For higher carrier density, the strong single-particle energy shifts lead to a reduction of the scattering efficiency. Additionally, at very high carrier densities the intradot processes are suppressed due to Pauli blocking. These effects result in a strong decrease of the single-particle broadening.

IV. CARRIER-PHONON INTERACTION

A. Theory

In this section, we compute correlation contributions in the optical spectra due to the interaction of carriers with LO phonons. In contrast to the frequently applied time-dependent perturbation theory, it has been pointed out in Ref. 18 that the interaction involving localized QD carriers requires a description in the polaron picture. In Ref. 19, quasiparticle renormalizations described by a polaronic retarded GF have been used within a quantum-kinetic theory to evaluate scattering processes and populations changes. We extend this treatment to the polarization dynamics to analyze the corresponding dephasing and interband-energy renormalizations.

Within the random-phase approximation (RPA) and the GKBA, the correlation contributions due to LO phonons are

$$\Gamma_{\alpha}^{\mathrm{DD}}(\hbar\omega) = i \sum_{\substack{a,b=e,h \\ b\neq a}} \sum_{\beta} \frac{M_{LO}^2}{e^2/\varepsilon_0} V_{\alpha\beta\alpha\beta} \times \{(1-f_{\beta}^{a})[(1+N_{\mathrm{LO}})G_{\beta,\alpha}^{a,b}(\hbar\omega - \hbar\omega_{\mathrm{LO}}) + N_{\mathrm{LO}}G_{\beta,\alpha}^{a,b}(\hbar\omega + \hbar\omega_{\mathrm{LO}})] + f_{\beta}^{a}[(1+N_{\mathrm{LO}}) \times G_{\beta,\alpha}^{a,b}(\hbar\omega + \hbar\omega_{\mathrm{LO}}) + N_{\mathrm{LO}}G_{\beta,\alpha}^{a,b}(\hbar\omega - \hbar\omega_{\mathrm{LO}})]\} \tag{10}$$

and

$$\Gamma_{\alpha\beta}^{\mathrm{OD}}(\hbar\omega) = i \sum_{\substack{a,b=e,h \\ b\neq a}} \frac{M_{LO}^2}{e^2/\varepsilon_0} V_{\alpha\beta\alpha\beta} \times \{(1-f_{\alpha}^{a})[(1+N_{\mathrm{LO}})G_{\beta,\alpha}^{b,a}(\hbar\omega - \hbar\omega_{\mathrm{LO}}) + N_{\mathrm{LO}}G_{\beta,\alpha}^{b,a}(\hbar\omega + \hbar\omega_{\mathrm{LO}})] + f_{\alpha}^{a}[(1+N_{\mathrm{LO}}) \times G_{\beta,\alpha}^{b,a}(\hbar\omega + \hbar\omega_{\mathrm{LO}}) + N_{\mathrm{LO}}G_{\beta,\alpha}^{b,a}(\hbar\omega - \hbar\omega_{\mathrm{LO}})]\}, \tag{11}$$

where the prefactor $M_{\mathrm{LO}}^2 = 4\pi\alpha(\hbar/\sqrt{2m})(\hbar\omega_{\mathrm{LO}})^{3/2}$ includes the polar coupling strength α, the reduced mass m, and the phonon energy $\hbar\omega_{\mathrm{LO}}$. In this equations we have introduced the abbreviation

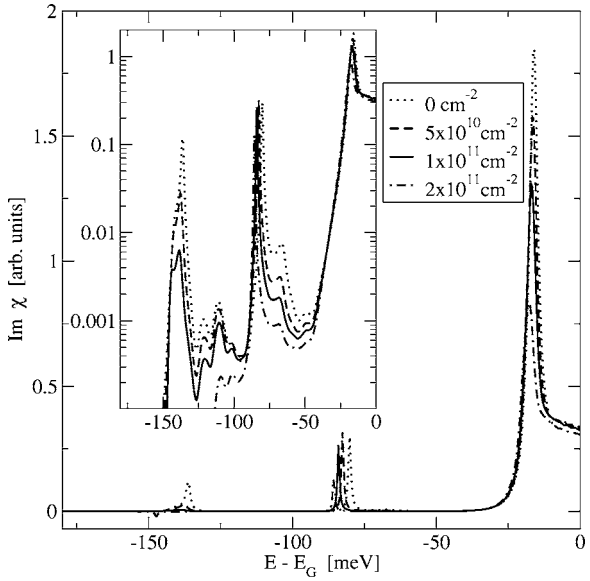

FIG. 5. The imaginary part of the optical susceptibility for the combined QD-WL system, including interaction-induced dephasing and line shifts due to the carrier-phonon interaction for various total carrier densities. The inset is a logarithmic plot of the QD resonances.

$$G_{\beta,\alpha}^{\mathrm{a,b}}(\omega) = \int d\tau\, e^{i\omega\tau} G_{\beta}^{a,\mathrm{ret}}(\tau) G_{\alpha}^{b,\mathrm{ret}}(\tau), \tag{12}$$

which represents the Fourier transform of a product of two retarded polaronic GFs. Please note that the structure of this quantity can be traced back to the change from the c,v picture to the e,h picture. Through these functions polaronic renormalization effects such as phonon replicas and hybridization between the localized states[19] are included in Eqs. (10) and (11). Details for the calculation of the retarded polaronic GF are give in Appendix B.

B. Results

The high-density spectra with dephasing due to the Coulomb interaction exhibit only three resonances, namely *s*-shell, *p*-shell, and the excitonic resonance of the WL. Absorption spectra with correlation contributions due to the interaction of carriers with LO phonons are shown in Fig. 5. Polaronic renormalizations of the single-particle states lead to a more complicated resonance structure for the interband transitions displayed in the inset of Fig. 5. One can identify phonon replicas and results of the hybridization of the single-particle states. For example, the *s*-shell resonances have a shoulder on the lower energetic side due to hybridization of the corresponding electron state. Energetically above the resonances of the *s* shell and the *p* shell, several peaks due to phonon replicas and their hybridizations can be observed. The non-Lorentzian character of the lineshapes is even more

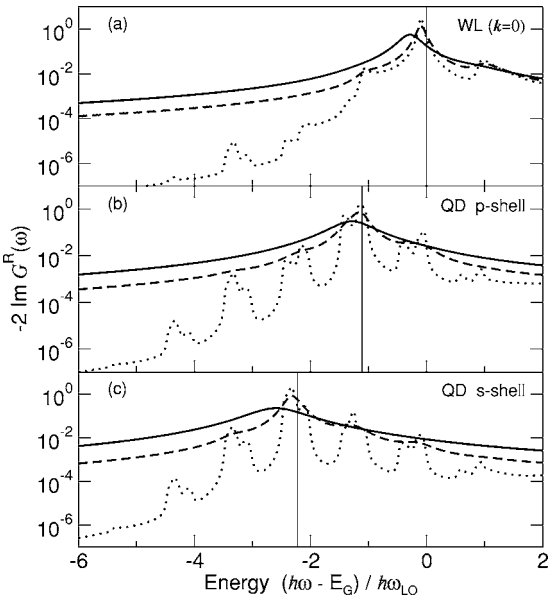

FIG. 6. Spectral function of the $k=0$ WL state and the QD p- and s-shell states, including the interaction with LO phonons and the Coulomb interaction of carriers. The total carrier density is 0 (dotted line), 5×10^8 cm^{-2} (dashed line), and 2×10^{11} cm^{-2} (solid line). Vertical lines indicate the free carrier energies.

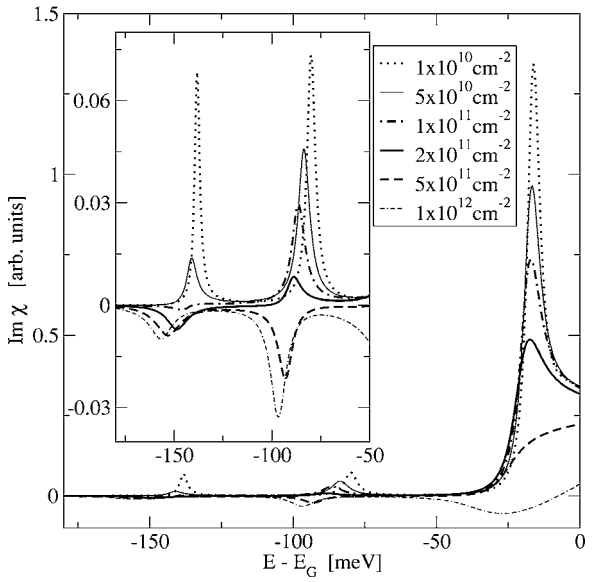

FIG. 7. Imaginary part of the optical susceptibility for the combined QD-WL system, including interaction-induced dephasing and line shifts due to the Coulomb interaction and the carrier-phonon interaction for various total carrier densities. The inset shows a scale-up of the QD resonances.

pronounced as for the spectra with Coulomb interaction. On the other hand, the damping of the resonances at higher densities remains weak.

V. DEPHASING DUE TO CARRIER-PHONON AND COULOMB INTERACTION

In this section, we investigate the combined influence of the carrier-carrier Coulomb scattering and the interaction of the carrier with LO phonons. It turns out that polaronic resonances in the single-particle spectral function are strongly damped out due to Coulomb scattering of carriers, even at low carrier densities, so that a pole approximation for the single-particle properties of the interacting system is reasonable. On the other hand, interband energy renormalizations and dephasing contributions due to the interaction of carriers with LO phonons continue to be important. Since our goal is a calculation of optical spectra for the QD-WL system under the influence of correlation effects at elevated carrier densities, we use for the description of single-particle properties a retarded GF obeying Eq. (B1) with the free carrier energy on the lhs replaced by $\tilde{\varepsilon}^a_\alpha = e^a_\alpha + \Delta^a_\alpha - i\gamma^a_\alpha$, which is determined by Eqs. (7) and (8). In other words the polaron is obtained by dressing with the phonon interaction, not the free particles but the quasiparticles obtained by Coulomb renormalization. Rewriting the retarded GF as

$$G^{a,\mathrm{ret}}_\alpha(\tau) = \mathcal{G}^a_\alpha(\tau) e^{-(i/\hbar)(\Delta^a_\alpha - i\gamma^a_\alpha)\tau}, \tag{13}$$

we separate in $\mathcal{G}^a_\alpha(\tau)$ the phonon renormalization effects, which are, of course, influenced by the presence of the Coulomb interaction. (The equation obeyed by $\mathcal{G}$ still contains Δ and γ.) The finite lifetime of these quasiparticles produces in general sufficient damping to reduce the polaronic GF $\mathcal{G}^a_\alpha$ to a single-pole structure. This pole is used instead of e^a_α in Eq. (7). In this way the Coulombian and the polaronic problems become coupled and have to be solved self-consistently. The iterative solution to this problem converges rapidly. Results of the spectral function of QD and WL states are shown in Fig. 6. Even for low carrier densities, polaronic structures are strongly broadened as a result of the dominant role of damping due to Coulomb scattering. [For low carrier densities the exponential decay $e^{-(\gamma^a_\alpha/\hbar)\tau}$ due to the Coulomb interaction, which is superimposed to the polaronic function $\mathcal{G}^a_\alpha(\tau)$ in Eq. (13), might somewhat overestimate the damping of the polaronic resonances. Nevertheless at higher carrier densities we expect a strong broadening of the polaron satellites.]

In Fig. 7 calculated absorption spectra are shown, which include correlations due to carrier-carrier scattering Eqs. (3) and (4), and the interaction with LO phonons, Eqs. (10) and (11), both evaluated with self-consistently renormalized single-particle energies. As in the result for dephasing due to the Coulomb interaction, Fig. 1, we see the bleaching and red shift of the resonances due to many-body interactions and also the saturation of the s-shell gain. Although we observe that the Coulomb interaction is the clearly dominant dephasing mechanism for high carrier densities, we also infer from a comparison of Fig. 7 with Fig. 1 that even in the gain regime the electron-phonon interaction gives rise to a clear increase in the dephasing. Nevertheless, polaronic features are absent in the spectra, since the complicated multipeak structure of the spectral function is completely damped out due to Coulomb effects.

For intermediate carrier densities around 5×10^{10} cm^{-2}, both types of interaction processes are equally important. Comparing the results in Fig. 8, one can conclude for our situation that taking only the Coulomb dephasing mechanism

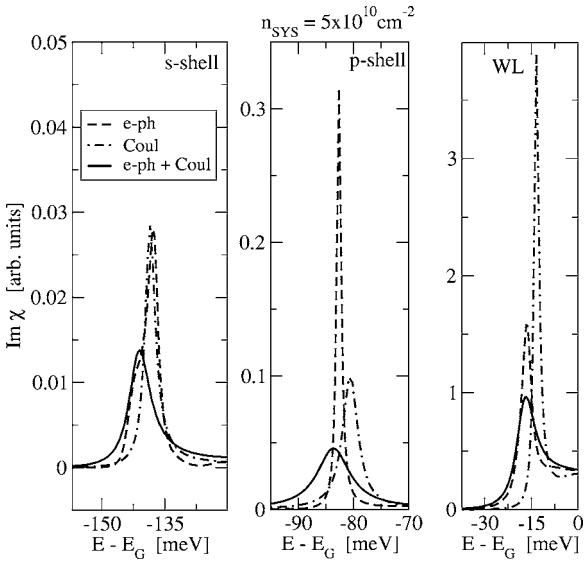

FIG. 8. A comparison of spectra with different dephasing mechanisms for a carrier density of 5×10^{10} cm^{-2}.

into account underestimates the dephasing of the ground state transition by roughly a factor of 2, while the damping of the WL is even dominated by a carrier-phonon interaction. For higher carrier densities, however, this picture changes, as can be seen in Fig. 9. Using a carrier density of 2×10^{11} cm^{-2}, the Coulomb interaction is clearly the dominant mechanism for the QD resonances. For the excitonic resonance of the WL, the two mechanisms are equally important, even at this rather high carrier density, where we are already in the gain regime for the *s*-shell transition.

Comparison with experiments

In most experiments, the emission from an ensemble of QDs is studied such that the additional inhomogeneous

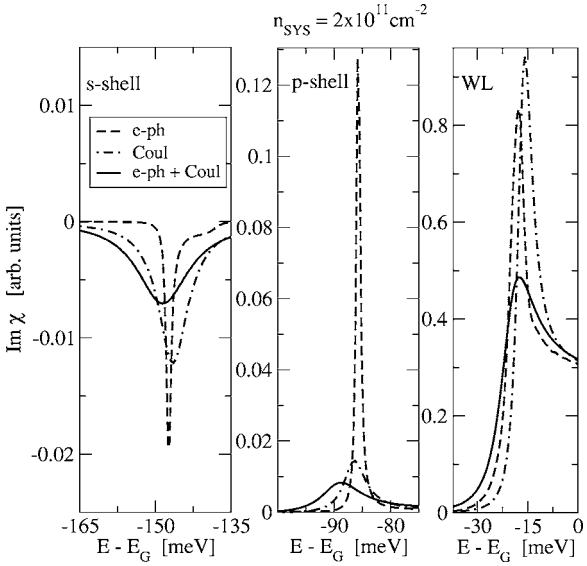

FIG. 9. A comparison of spectra with different dephasing mechanisms for a carrier density of 2×10^{11} cm^{-2}.

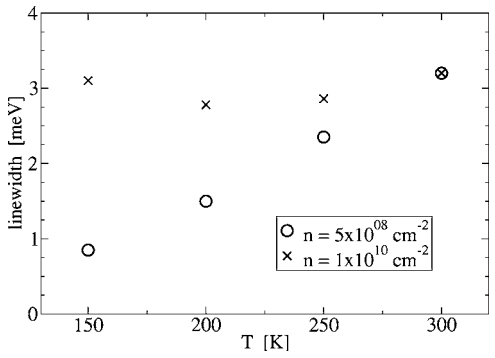

FIG. 10. Temperature dependence of the linewidth (full half-width) for the QD ground state resonance and different carrier densities.

broadening of the QD resonances due to size and composition fluctuations contributes. However, recent experiments[20,21] have been performed at room temperature on single QDs. In Fig. 1(a) of Ref. 21, optical spectra are displayed for different excitation intensities. Although a direct comparison of the excitation dependence is not possible, due to uncertainties in the carrier densities generated in those experiments, the general features of the spectra are identical. A clear distinction between the QD transitions and the excitonic resonance of the WL is seen. The QD resonances show a density-dependent bleaching and a pronounced red shift due to many-body correlations, while the spectral position of the WL is almost unchanged and the WL resonance is only bleached out. This means that the red shift of the QD resonances cannot be attributed to bandgap shrinkage effects of the WL.

The observed homogeneous linewidth in this experiment is 8–13 meV, depending on the excitation intensity. This is larger than our findings, but one has to take into account that the QD, investigated in Ref. 21, seems to have three confined electronic shells, which results in more dephasing channels. A better comparison is possible with the results of Ref. 20 because two types of QDs are investigated, where one type resembles our model in the respect that it is supposed to have two confined electronic shells. Regarding the *s* shell, we can infer from Fig. 3 of Ref. 20 that the observed homogeneous linewidth is slightly above 3 meV at room temperature, which is similar to our result of 3.2 meV. The calculated value is practically unchanged for a carrier density range from 5×10^{8} to 10^{10} cm^{-2}.

For a better comparison with experiments, we have also calculated the temperature dependence of the homogeneous linewidth in a temperature range in which the influence of LA phonons remains small. As shown in Fig. 10, we obtain for low carrier densities (where carrier-carrier scattering is sufficiently weak), the expected reduction of dephasing with decreasing temperature, as seen in Ref. 20. (A quantitative comparison would require a better knowledge of QD parameters and phonon modes in the QD-WL system.) For the case of a higher excitation density of 10^{10} cm^{-2}, the line broadening is almost temperature independent, due to a balancing of different scattering channels. The dephasing due to LO phonons decreases with temperature, as in the low-density

case. However, the Coulomb interaction is no longer negligible for this carrier density. With decreasing temperature, the WL states are less populated while the occupation of QD states increases. This enhances intradot relaxation processes and provides stronger dephasing due to the Coulomb interaction.

VI. CONCLUSION

We have calculated the excitation-induced dephasing and line shifts for a QD-WL system on a microscopic basis. Both Coulomb and LO-phonon contributions to the homogeneous linewidths are found to be equally important for elevated carrier densities. The role of self-consistent single-particle energy renormalizations in the scattering integrals is emphasized. For the Coulomb interaction the relative importance of various scattering channels has been analyzed.

ACKNOWLEDGMENTS

This work was supported by the Deutsche Forschungsgemeinschaft and with a grant for CPU time at the NIC, Forschungszentrum Jülich.

APPENDIX A: QUANTUM DOT MODEL SYSTEM AND COULOMB MATRIX ELEMENTS

We focus on lens-shaped InGaAs QDs that are located on top of a two-dimensional WL. Such systems typically consist of localized QD states energetically below a quasicontinuum of delocalized WL states for electrons and holes. In the present paper we assume the single-particle spectrum, as depicted in Fig. 1 of Ref. 27. For the in-plane motion we assume a parabolic confinement potential, leading to a harmonic oscillator like single-particle wave functions. To account for the finite depth of the confinement potential, we take into account two confined shells for electrons and holes, which we refer to as s shell for the ground state and a p shell for the double degenerated excited state, due to their angular momentum properties. We choose a level spacing of 40 meV for electrons and 15 meV for holes so that the free carrier transitions appear at −55 meV relative to the WL band edge for the p shell and at −110 meV for the s shell. The WL states are modeled by orthogonalized plane waves (OPW).[27] For the motion in the growth direction (the z direction), we assume an infinite height potential well of 4 nm thickness.

Under this assumptions we can construct the Coulomb matrix elements,

$$V_{\alpha\beta\gamma\delta} = \frac{1}{A}\sum_{\mathbf{q}} V_{\mathbf{q}} \times \int d^2\varrho\, \varphi_\alpha^*(\varrho)\varphi_\delta(\varrho)e^{-i\mathbf{q}\cdot\varrho} \times \int d^2\varrho'\, \varphi_\beta^*(\varrho')\varphi_\gamma(\varrho')e^{i\mathbf{q}\cdot\varrho'}, \tag{A1}$$

consisting of overlap integrals between single-particle wave functions and the Coulomb potential $V_{\mathbf{q}}$, as given in Ref. 27. For the screening we use a generalization of the static Lindhard formula, which is also explained in detail in Ref. 27. This procedure leads to the replacement $V_{\mathbf{q}} \rightarrow W_{\mathbf{q}}$ in Eq. (A1) for the matrix elements $W_{\alpha\beta\gamma\delta}$. Because we are working in the envelope approximation with equal envelope wave functions, we do not need to consider band indices for the Coulomb matrix elements. All other parameters are chosen as in Ref. 27.

APPENDIX B: RETARDED POLARONIC GREEN'S FUNCTION

The retarded polaronic GFs obeys the equation of motion,

$$\left(i\hbar\frac{\partial}{\partial\tau} - e_\alpha^a\right)G_\alpha^{a,\mathrm{ret}}(\tau) = \delta(\tau) + \int d\tau'\, \Sigma_\alpha^{a,\mathrm{ret}}(\tau-\tau')G_\alpha^{a,\mathrm{ret}}(\tau'). \tag{B1}$$

The corresponding retarded self-energy is given in RPA by

$$\Sigma_\alpha^{a,\mathrm{ret}}(\tau) = i\hbar\sum_\beta G_\beta^{a,\mathrm{ret}}(\tau)D_{\beta\alpha}^<(-\tau). \tag{B2}$$

We assume for the calculations restricted to electron-phonon interaction that the polaronic retarded GF is not influenced by population effects. This has been verified for a bulk system in Ref. 28.

Assuming that the phonon system is in thermal equilibrium, the phonon propagator (combined with the interaction matrix elements) is given by

$$i\hbar\, D_{\beta\alpha}^<(\tau) = \frac{M_{LO}^2}{e^2/\varepsilon_0}V_{\beta\alpha\beta\alpha} \times [N_{\mathrm{LO}}e^{-i\omega_{\mathrm{LO}}\tau} + (1+N_{\mathrm{LO}})e^{i\omega_{\mathrm{LO}}\tau}], \tag{B3}$$

where we consider monochromatic LO phonons with the frequency ω_{LO}. The corresponding population of the phonon bath is given by a Bose-Einstein distribution, $n_{\mathrm{LO}} = 1/(e^{\hbar\omega_{\mathrm{LO}}/kT}-1)$, and $V_{\beta\alpha\beta\alpha}$ is the unscreened Coulomb matrix element (cf. Appendix A).

APPENDIX C: CONNECTION BETWEEN MEMORY EFFECTS AND FREQUENCY DEPENDENCE IN THE SCATTERING INTEGRALS

In this section we is show how the non-Markovian (Markovian) scattering integrals lead to frequency-dependent (independent) dephasing terms. The time domain formulation of the SBE with correlation contributions due to Coulomb interaction is given by[22]

$$\left(i\hbar\frac{\partial}{\partial t} - \varepsilon_\alpha^{e,\mathrm{HF}} - \varepsilon_\alpha^{h,\mathrm{HF}}\right)\psi_\alpha(t) + [1-f_\alpha^e - f_\alpha^h]\Omega_\alpha^{\mathrm{HF}}(t) = -i\hbar\, S_\alpha^{\mathrm{Coul}}(t). \tag{C1}$$

In the following we explicitly consider the direct e-e and h-h interaction contributions of the diagonal dephasing:

$$S_\alpha(t) = \hbar^2\int_{-\infty}^t dt' \sum_{\substack{a,b=e,h \\ b\neq a}}\sum_{\alpha_1\alpha_2\alpha_3} 2W_{\alpha\alpha_2\alpha_3\alpha_1}(t)W^*_{\alpha\alpha_2\alpha_3\alpha_1}(t') \times G_\alpha^{b,\mathrm{ret}}(t,t') \times [G_{\alpha_2}^{a,\mathrm{ret}}(t,t')]^* G_{\alpha_3}^{a,\mathrm{ret}}(t,t')G_{\alpha_1}^{a,\mathrm{ret}}(t,t')\psi_\alpha(t')F_{\alpha_2\alpha_3\alpha_1}(t'). \tag{C2}$$

Other terms can be treated in complete analogy. Here we have defined

$$F_{\alpha_2\alpha_3\alpha_1}(t) = [1 - f^a_{\alpha_2}(t)] f^a_{\alpha_3}(t) f^a_{\alpha_1}(t) + (f \to 1 - f). \quad \text{(C3)}$$

We assume static screening where the Coulomb matrix elements depend only parametrically on time via the population functions. For the discussed excitation conditions, both f and W are time independent. With the ansatz

$$G^{a,\mathrm{ret}}_{\alpha}(t,t') = -\frac{i}{\hbar}\Theta(t-t')e^{-(i/\hbar)\tilde{\varepsilon}^a_\alpha(t-t')}, \quad \text{(C4)}$$

which corresponds to Eq. (6), we obtain

$$S_\alpha(t) = \frac{1}{\hbar^2}\sum_{\substack{a,b=e,h \\ b\neq a}}\sum_{\alpha_1\alpha_2\alpha_3} 2W_{\alpha\alpha_2\alpha_3\alpha_1}W^*_{\alpha\alpha_2\alpha_3\alpha_1}F_{\alpha_2\alpha_3\alpha_1}$$

$$\times \int_{-\infty}^{t} dt'\, e^{-(i/\hbar)(\tilde{\varepsilon}^b_\alpha + \tilde{\varepsilon}^a_{\alpha_1} - (\tilde{\varepsilon}^a_{\alpha_2})^* + \tilde{\varepsilon}^a_{\alpha_3})(t-t')}\psi_\alpha(t').$$

With the Fourier transform $\psi_\alpha(t) = \int (d\omega/2\pi)e^{-i\omega t}\psi_\alpha(\omega)$, and using the integral relation

$$\int_{-\infty}^{t} dt'\, e^{(i/\hbar)\Delta(t-t')} = \frac{i\hbar}{\Delta}, \quad \mathrm{Im}\,\Delta > 0, \quad \text{(C5)}$$

we arrive at Eq. (1) and the terms of Eq. (3), which are discussed here.

For the Markov approximation, one separates from the transition amplitude a phase factor, which rapidly oscillates with the (renormalized) interband transition energy, via the ansatz

$$\psi_\alpha(t) = e^{(i/\hbar)(\tilde{\varepsilon}^e_\alpha + \tilde{\varepsilon}^h_\alpha)t}\tilde{\psi}_\alpha(t). \quad \text{(C6)}$$

Now one assumes that a weakly time-dependent $\tilde{\psi}_\alpha(t')$ can be replaced by the transition amplitude at the actual time t, $\tilde{\psi}_\alpha(t)$, thus neglecting the memory effects of $\tilde{\psi}_\alpha$. Using the integral relation (C5) again, one arrives at a expression similar to Eq. (3), but with $g[\hbar\omega - \tilde{\varepsilon}^b_\alpha - \tilde{\varepsilon}^a_{\alpha_1} + (\tilde{\varepsilon}^a_{\alpha_2})^* - \tilde{\varepsilon}^a_{\alpha_3}]$ replaced by $g[\tilde{\varepsilon}^a_\alpha - \tilde{\varepsilon}^a_{\alpha_1} + (\tilde{\varepsilon}^a_{\alpha_2})^* - \tilde{\varepsilon}^a_{\alpha_3}]$.

*Electronic addess: www.itp.uni-bremen.de/ag-jahnke/

[1] Y. Masumoto and T. Takagahara, in *Semiconductor Quantum Dots*, 1st ed. (Springer-Verlag, Berlin, 2002).

[2] P. Michler, in *Single Quantum Dots*, 1st ed. (Springer-Verlag, Berlin, 2003).

[3] P. Michler, A. Imamoglu, M. D. Mason, P. J. Carson, G. F. Strouse, and S. K. Buratto, Nature **406**, 968 (2000).

[4] E. Moreau, I. Robert, L. Manin, V. Thierry-Mieg, J. M. Gerard, and I. Abram, Phys. Rev. Lett. **87**, 183601 (2001).

[5] M. Pelton, C. Santori, J. Vuckovic, B. Zhang, G. S. Solomon, J. Plant, and Y. Yamamoto, Phys. Rev. Lett. **89**, 233602 (2002).

[6] J. P. Reithmaier, G. Sek, A. Löffler, C. Hofmann, S. Kuhn, S. Reitzenstein, L. V. Keldysh, V. D. Kulakovskii, T. L. Reinecke, and A. Forchel, Nature **432**, 197 (2004).

[7] T. Yoshie, A. Scherer, J. Hendrickson, G. Khitrova, H. M. Gibbs, G. Rupper, C. Ell, O. B. Shchekin, and D. G. Deppe, Nature **432**, 200 (2004).

[8] Y. Z. Hu, H. Gießen, N. Peyghambarian, and S. W. Koch, Phys. Rev. B **53**, 4814 (1996).

[9] H. C. Schneider, W. W. Chow, and S. W. Koch, Phys. Rev. B **64**, 115315 (2001).

[10] H. C. Schneider, W. W. Chow, and S. W. Koch, Phys. Rev. B **70**, 235308 (2004).

[11] G. Manzke and K. Henneberger, Phys. Status Solidi B **234**, 233 (2002).

[12] A. V. Uskov, A.-P. Jauho, B. Tromborg, J. Mørk, and R. Lang, Phys. Rev. Lett. **85**, 1516 (2000).

[13] B. Krummheuer, V. M. Axt, and T. Kuhn, Phys. Rev. B **65**, 195313 (2002).

[14] E. A. Muljarov and R. Zimmermann, Phys. Rev. Lett. **93**, 237401 (2004).

[15] P. Borri, W. Langbein, S. Schneider, U. Woggon, R. L. Sellin, D. Ouyang, and D. Bimberg, Phys. Rev. Lett. **87**, 157401 (2001).

[16] H. Htoon, D. Kulik, O. Baklenov, A. L. Holmes, Jr., T. Takagahara, and C. K. Shih, Phys. Rev. B **63**, 241303(R) (2001).

[17] R. Oulton, J. J. Finley, A. I. Tartakovskii, D. J. Mowbray, M. S. Skolnick, M. Hopkinson, A. Vasanelli, R. Ferreira, and G. Bastard, Phys. Rev. B **68**, 235301 (2003).

[18] T. Inoshita and H. Sakaki, Phys. Rev. B **56**, R4355 (1997).

[19] J. Seebeck, T. R. Nielsen, P. Gartner, and F. Jahnke, Phys. Rev. B **71**, 125327 (2005).

[20] M. Bayer and A. Forchel, Phys. Rev. B **65**, 041308(R) (2002).

[21] K. Matsuda, K. Ikeda, T. Saiki, H. Saito, and K. Nishi, Appl. Phys. Lett. **83**, 2250 (2003).

[22] H. Haug and S. W. Koch, *Quantum Theory of the Optical and Electronic Properties of Semiconductors*, 3rd ed. (World Scientific, Singapore, 1994).

[23] F. Jahnke, M. Kira, and S. W. Koch, Z. Phys. B: Condens. Matter **104**, 559 (1997).

[24] T. R. Nielsen, P. Gartner, M. Lorke, J. Seebeck, and F. Jahnke, Phys. Rev. B **72**, 235311 (2005).

[25] P. Lipavský, V. Špička, and B. Velický, Phys. Rev. B **34**, 6933 (1986).

[26] H. C. Tso and N. J. MorgensternHoring, Phys. Rev. B **44**, 1451 (1991).

[27] T. R. Nielsen, P. Gartner, and F. Jahnke, Phys. Rev. B **69**, 235314 (2004).

[28] P. Gartner, L. Bányai, and H. Haug, Phys. Rev. B **60**, 14234 (1999).